Article

Not peer-reviewed version

Advanced Platelet Lysate Aerogels: Biomaterials for Regenerative Applications

Fahd Tibourtine , Thibault Canceill , Andrea Marfoglia , Philippe Lavalle , Laure Gibot , Ludovic Pilloux , Claire Medemblik , Dominique Goudouneche , Agnès Dupret-Bories * , Sophie Cazalbou *

Posted Date: 3 January 2024

doi: 10.20944/preprints202401.0132.v1

Keywords: Human Platelet lysate; supercritical carbon dioxide; Advanced Therapy Medicinal Products (ATMP); gels; regenerative medecine

Article

Advanced Platelet Lysate Aerogels: Biomaterials for Regenerative Applications

Fahd Tibourtine [1], Thibault Canceill [2], Andrea Marfoglia [1,3], Philippe Lavalle [4], Laure Gibot [5], Ludovic pilloux [3], Claire Medemblik [4], Dominique Goudouneche [6], Agnes Dupret Bories [1,7,8] and Sophie Cazalbou [1,*]

[1] CIRIMAT, Université Toulouse 3 Paul Sabatier, Toulouse INP, CNRS, Université de Toulouse, 118 Route de Narbonne, 31062 Toulouse cedex 9 - France
[2] Département Odontologie, Faculté de Santé, Hôpitaux de Toulouse, Université Paul Sabatier, 3 Chemin des Maraichers, 31062 Toulouse Cedex 9, France
[3] Laboratoire de Génie Chimique, Université Toulouse 3 Paul Sabatier, Toulouse INP, CNRS, Université de Toulouse, 31062 Toulouse, France.
[4] Institut National de la Santé et de la Recherche Médicale, Inserm UMR_S 1121 Biomaterials and Bioengineering.
[5] Laboratoire Softmat, Université de Toulouse, CNRS UMR 5623, Université Toulouse III – Paul Sabatier, France.
[6] Centre de Microscopie Electronique Appliquée à la Biologie, Faculté de Médecine, Toulouse, France
[7] Department of Surgery, University Cancer Instituteof Toulouse – Oncopole, 1 Avenue Irène Joliot-Curie,31100 Toulouse, France.
[8] Department of Ear, Nose and Throat Surgery, Toulouse University Hospital – Larrey Hospital, Toulouse, France.
* Correspondence: sophie.cazalbou@univ-tlse3.fr

Abstract: Human Platelet lysate, a hemoderivative product rich in growth factors, holds significant promise in tissue engineering and regenerative medicine. However, its practical utility in liquid or gel form is hampered by challenges such as limited stability and handling difficulties. This study aimed to engineer dry and porous aerogels from platelet lysate hydrogel using an environmentally friendly supercritical CO_2-based shaping process customized for tissue engineering applications. The resulting aerogels demonstrated remarkable mechanical robustness and improved manageability. Notably, they exhibited a high-water absorption capacity. Moreover, these aerogels exhibited a sustained and favourable biological response *in-vitro*. They demonstrated the ability to release functional growth factors, sustaining cellular metabolic activity similar to that of conventional culture conditions, even after prolonged storage. Furthermore, they supported the adhesion and proliferation of murine fibroblasts (BALB-3T3) and the migration of Human Umbilical Vein Endothelial Cells (HUVEC). In addition to serving as excellent matrices for cell culture, these proposed aerogels also function as efficient growth factor delivery systems. This multifunctional capability positions them as promising candidates for various tissue regeneration strategies. Importantly, the elaborated aerogels can be conveniently stored and considered as ready-to-use products, enhancing their practicality and applicability in regenerative medicine

Keywords: Human Platelet lysate; supercritical carbon dioxide; aerogel; tissue repair; biomaterials Advanced Therapy Medicinal Products (ATMP)

1. Introduction

Platelets are circulating anucleate cell fragments in the blood that play a crucial role in the process of coagulation and the beginning of wound healing [1]. In case of injury, platelets aggregate onto the wounded vessel walls and activate to form a blood clot to prevent blood loss at the site of injury [2]. Besides their primary role in hemostasis and thrombosis, platelets participate in numerous other physiological and pathological processes, including but not limited to inflammation, wound healing, tumor metastasis, and angiogenesis, *via* the secretion of different bioactive molecules such

 doi:10.20944/preprints202401.0132.v1

as growth factors, coagulation factors, adhesion molecules, and chemokines stored initially in their alpha granules, the principal storage granule of platelets [3].

Recently, several studies have focused on the design of hemoderivative biomaterials based on platelet derivatives such as platelet-rich plasma (PRP) and platelet lysate (PL) as they have great potential for regenerative therapy as autologous sources of growth factors [4]. They can be obtained using simple and cost-effective procedures and used in personalized medicine approaches. The autologous application of endogenous growth factors considerably reduces the risks of disease transmission and simultaneously allows for the induction of the "wound healing cascade" in a physiological manner.

Human Platelet Lysate (hPL) is derived from human platelet concentrates through mechanical or chemical disruption of platelet membranes [5]. Growth factors (GFs) such as insulin-like growth factor-1 (IGF-I), platelet-derived growth factor (PDGF), vascular endothelial growth factor (VEGF), fibroblast growth factor (FGF), epidermal growth factor (EGF), platelet-derived epidermal growth factor (PDEGF) have been identified in it [6]. These growth factors play crucial roles in different stages of wound healing, such as chemotaxis [7], angiogenesis [8] ,cell proliferation and differentiation [9,10].

Previous studies have shown that it can be applied as an effective source of growth factors for tissue regeneration, such as for tendon [11], bone [12], cartilage [13], skin [14]and other organs [15]. It has also been demonstrated that hPL would be more suitable for cell culture as a medium supplement compared to other animal-derived products such as fetal bovine serum [5].

In clinical applications, hPL is often applied externally to the target organ (e.g., cornea, diabetic foot ulcer…)[16], added to an implanted material [17] or injected directly into the lesion [18]. It is used either alone as a source of growth factors [19] or as a scaffold for the simultaneous delivery of cells(e.g., Mesenchymal Stem Cell)[20]. Indeed, once associated with calcium, the PL coagulates and thus forms a hydrogel. However, the hydrogels obtained present low mechanical properties, which result in a lack of rigidity and a tendency to adhere to surfaces, making them very challenging to handle[21]. Several studies have proposed various strategies to overcome this limitation including the incorporation of additional materials to enhance rigidity [22][23]. Moreover, their high-water content limits their storage duration [24], thereby adding an additional constraint to their use.

To overcome these limitations, in this article we propose the design of a dry and porous biomaterial offering improved properties in terms of handling properties and stability. This material presented in the form of an aerogel rich in human platelet lysate (hPL). Is obtained from hPL hydrogel dried by a process involving the use of supercritical carbon dioxide ($scCO_2$). $ScCO_2$ is a known method for preparing aerogels. It offers several advantages such as availability, non-toxicity, non-flammability, and low cost. It also confers the ability to regulate pore size, produce monolithic and solvent-free aerogels [25].

The use of aerogels in the biomedical domain has witnessed substantial advancement due to their numerous notable benefits. These include their capacity to retain a porous structure, exhibit superior mechanical strength, and maintain long-term stability. Furthermore, biopolymer-based aerogels are distinguished for their outstanding biocompatibility and biodegradability, and their potential for serving as drug delivery systems [26].

The development of human-derived aerogels offers a range of significant clinical advantages, enhancing their relevance for applications in regenerative medicine. Their ability to facilitate enhanced tissue regeneration stems primarily from the presence of multiple bioactive molecules within these materials, creating an environment conducive to cellular regeneration and tissue restoration. Importantly, their use also reduces the risk of disease transmission compared to animal-derived biomaterials. Their dry form confers a substantial advantage in a clinical setting, facilitating their handling, long-term storage, and immediate availability. This feature, combined with their capacity to induce a positive biological response, opens promising prospects for versatile clinical applications, including the regeneration of tissues such as skin, bone, and cartilage. These aerogels stand out for their ability to deliver growth factors, significantly enhancing the regeneration process.

Preprints (www.preprints.org) | NOT PEER-REVIEWED | Posted: 3 January 2024 doi:10.20944/preprints202401.0132.v1

2. Materials and Methods

2.1. Aerogel preparation

2.1.1. Synthesis of Human Platelet lysate Hydrogel:

The platelet lysate hydrogel was prepared by combining Human Platelet Lysate (hPL) (Human PL100®, MacoPharma, France) with the following components: sodium chloride (NaCl) (Fisher scientific, Loughborough, United Kingdom) at a concentration of 0.9% (w/v), tranexamic acid at 0.1 g/mL (Acros Organics, Geel, Belgium) , and anhydrous calcium chloride ($CaCl_2$) at 10% (w/v) (Fisher Scientific, Illkirch, France). The hPL solution accounted for 68.7% (v/v) of the total volume of the preparation, while $CaCl_2$ constituted 2.5%(v/v), NaCl 28.6%(v/v), and tranexamic acid 0.2%(v/v). Precise volumes of each constituent were calculated to achieve a final volume of 2 mL for the solution. The mixture was incubated at 37°C for 30 minutes in cylindrical containers which enabled formation of hydrogel cylinders (approximately 1.8 cm in diameter and 1cm in height).

2.1.2. Water-Solvent Exchange of Hydrogel

Once formed, and prior to the drying process, the hydrogels were dehydrated in successive baths of 24h in increasing concentrations of acetone (25%, 50%, 75% and 100%). The volume (500 mL) of acetone used is largely sufficient in volume to ensure that the water released by the hydrogel does not significantly modify the acetone concentration of the exchange solution. 48 hours have been added to the 100% acetone baths to guarantee that the acetone water exchange is complete and obtention of an organogel (Figure 1))[27].

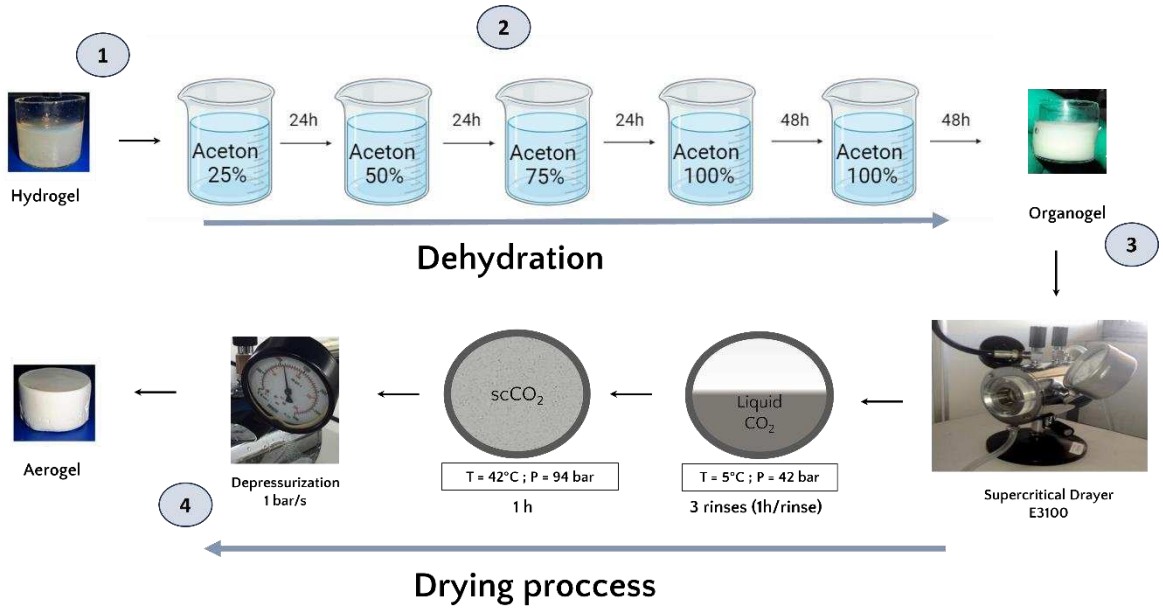

Figure 1. (1) The hPL hydrogel precursor. (2) Schematic representation of the acetone bath steps involved in the formation of the organogel and the subsequent dehydration and substitution of the aqueous phase with an organic phase miscible in liquid CO_2. (3) Schematic illustration of the supercritical CO_2 drying process. (4) The final product, the platelet lysate aerogel.

2.1.3. Aerogel production by supercritical CO_2 drying

The organogels were placed in the supercritical CO_2 chamber ((E3100 Critical Point Dryer, Quorum Technologies Ltd, UK) and once the chamber was closed, it was filled halfway with liquid CO_2 in temperature 5 °C to reach a pressure of 42 bar for one hour to ensure acetone-liquid CO_2 exchange.

 doi:10.20944/preprints202401.0132.v1

After one hour of incubation, a depressurization was performed to remove the liquid CO_2 mixed with acetone and replaced with fresh liquid CO_2. This process was repeated 3 times. Then, the system was brought to the supercritical state by filling the chamber halfway with liquid CO_2 followed by an increase in temperature to 42°C which increased the pressure to 94 bar and reached the supercritical phase. These conditions were maintained for one hour. Finally, the top valve of the dryer was opened for one hour at a rate of 1 bar/sec to ensure a smooth release of the CO_2. In the end, the dryer was opened and the aerogels were collected.

2.2. Characterization of the aerogels

Different characterizations were performed in order to evaluate the effect of the shaping process involving $scCO_2$ on the physicochemical and bioactive properties of hPL aerogels. A comparison between hPL aerogels and hPL hydrogels fresh or dried at 37°C for 72h in a thermostatic oven was performed. The details of the techniques and parameters used are as follows:

2.2.1. Scanning electron microscopy

The morphology and microstructure of the aerogels were compared to fresh hPL hydrogels and oven-dried hPL hydrogels using scanning electron microscopy (SEM), (Quanta 250 FEG FEI, Thermo Scientific, USA).

The hPL hydrogels were formed as described above, then fixed overnight in 2% glutaraldehyde. After fixation, samples were dehydrated with ethanol gradient and treated with hexamethyldisilazane (HDMS)[28].

All samples were coated with 6 nm of platinum layer and observations were made in the secondary electron emission mode with high voltage of 5 kV.

2.2.2. Mercury Porosimetry

The porosity of the aerogels was measured using a mercury intrusion porosimeter (AutoPore III, Micromeritics Instruments Inc., Norcross, GA), which allows detection of pores in the range 360 µm to 4 nm. The pore size distribution was calculated as the differential mercury intrusion volume plotted versus the pore size. The total percentage porosity was calculated by Eq.(1):

$$P_{tot} = d_{app} * V_{Hg} * 100 \quad (1)$$

where d_{app} is the apparent density of the scaffold and V_{Hg} is the total mercury intrusion volume per gram of specimen analyzed. Each value was calculated from three parallel measurements (n=3).

2.2.3. Fourier Transform Infra-Red (FTIR) spectroscopy:

Attenuated total reflection Fourier transform infrared (ATR-FTIR) chemical analysis of hPL aerogels and liquid hPL was conducted at room temperature for the qualitative determination of bonds presented in samples.

For each spectrum, 64 scans between 400 and 4000 cm^{-1} were recorded, with a resolution of 4 cm^{-1} (Nicolet 5700, Thermo electron, USA).

2.2.4. Hydratation test

The aerogels were weighed. Then the samples were immersed in an aqueous medium (phosphate-buffered saline (PBS), pH=7.4) at 37°C to mimic physiological conditions.

Hydration measurements were conducted at various time intervals, specifically at 0, 5, 10, 15, 20, 25, 30, 35, 60, 120, 180, 240, 300, and 360 minutes. Following each designated time interval, the samples were carefully retrieved, excess surface liquid was removed, and the scaffolds were reweighed. The hydratation ratio of was defined as the ratio of the wet sample weight (W) to the initial dry sample weight (W_0), see Eq. (2) :

$$\text{Hydratation Ratio} = W/W_0 \quad [-] \quad (2)$$

The liquid content was investigated as the amount of liquid absorbed by the hydratation, as expressed in Eq.(3), where (W) is the wet sample weight and (W_0) is the dry sample weight:

 doi:10.20944/preprints202401.0132.v1

$$\text{Percentage of water content} = (W\text{-}W_0)/W_0.100\ [\%] \quad (3)$$

Each value was calculated from three parallel measurements (n=3).

2.2.5. Water drop contact angle

In order to investigate the hydrophobic/ hydrophilic properties, contact angles measurements were performed using the Drop Shape Analyzer DSA30S (KRÜSS GmbH, Germany). A calibrated 2µL droplet of PBS solutions, adjusted to pH 7.4 and maintained at temperature of 25°C, was dispensed using a fine needle and a carefully placed onto the surface of the samples. The contact angle, formed between the droplet and the surface of samples, was subsequently measured from the captured images using the KRÜSS advance software. This procedure was repeated three times on three different samples, and the behaviour of the droplet was assed until its complete absorption.

2.2.6. Texture profile analysis (TPA)

hPL hydrogels and hPL aerogels (cylindrical samples: 9 mm height, 16mm diameter) were tested under a double compression using a TA. XT Plus Texture Analyzer, (Texture Technologies, USA) equipped with a 6 mm diameter cylinder probe and a 5 kg load cell. The samples were placed on the base plate of the texture analyser and compressed at the speed of 0,5mm/sec to a deformation of 50%. The prop was then withdrawn from the sample at the speed of 0,5 mm/sec. The hardness and adhesiveness were measured for each sample (n=5) using texture Exponent 32 software (Texture Exponent 32 4.0, Stable Micro Systems Ltd, UK).

2.2.7. Quantification and kinetic release of total protein

The Pierce BCA protein assay kit (Thermo Scientific, USA) was used to quantify the total protein released from hPL aerogels and hPL hydrogels following the protocol provided for microplate assays. Samples were placed in 5mL of PBS (37°C, pH 7,4), aliquots of 500 µL were collected at 0, 1, 2, 4, 24 ,28 ,44 ,48 ,52, 72 and 168 hours. An equal volume of fresh PBS was added to the suspension to replace the collected samples, which were stored at -20°C until analysis. To assess the amount of total protein in the hPL stock solution, hPL was diluted at 1:20 in PBS to achieve a concentration range corresponding to the standards. Standards were prepared according to the manufacturer's protocol, and total protein was measured via absorbance at 560 nm using multi-well reader (CLARIOstar Plus, BMG Labtech, Germany). Data are presented as mean ± standard deviation for independent samples at each time point (n=3).

2.2.8. Quantification and kinetic release of VEGF by Enzyme Linked Immuno-Sorbent Assay (ELISA)

The release of VEGF from hPL aerogels was determined by enzyme-linked immunosorbent assay (Human VEGF Pre-Coated ELISA Kit,Biogems, USA), following the supplier's protocol. The optical density was read at 450nm using a multi-well plate reader.

The aerogels were immersed in 2 mL of PBS at 37°C and pH7,4 at predetermined time points (2, 4, 8, 24, 48 and 120 hours), aliquots of 150 µL were collected and stored at -20°C. The analysis was performed in triplicate (n=3).

2.3. In-vitro biological studies

2.3.1. Metabolic activity measurement by MTT assay

To assess the integrity and functionality of growth factors released by hPL aerogels, viability of cells exposed to medium conditioned by hPL aerogels was evaluated using the MTT assay method [29] based on the following principle:

BALB-3T3 fibroblasts cells were seeded at a population density of 9000 cells in 100µL per well in a 96-well plate in 100 µL of Dulbecco's Modified Eagle Medium (HyClone™ DMEM) supplemented with 10% Fetal Bovine Serum (FBS)(HyClone™), penicillin (100 U/mL) and

 doi:10.20944/preprints202401.0132.v1

streptomycin (100 mg/mL) (Sigma-Aldrich Chemical Co. Saint-Quentin-Fallavier, France). After 24 hours of incubation, the culture medium was replaced with 100 µL of extract medium obtained from the foams. The extract medium was prepared by incubating the foams in DMEM without FBS for 24 hours. The volume of DMEM used to incubate the aerogels was calculated so that the medium would be supplemented with 10% hPL (e.g. if 1 mL of hPL was used to prepare the aerogel, it would be put in 10 mL of DMEM). They were treated with conditioned medium previously in contact with the materials for 24 hours.

As a positive control, DMEM medium supplemented with 10% FBS was used and for the negative control 20% dimethylsulfoxide (DMSO) was used. A control of DMEM alone without FBS was used to assess the growth factors effect.

After 24 hours of incubation with the extract medium, the medium was removed and replaced with 100 µL of MTT solution (final concentration 1 mg/mL) prepared in DMEM medium.

The plates were then incubated at 37°C for 2 hours in a humidified atmosphere with 5% CO_2. MTT solution and formazan crystals were dissolved in 100 µL of DMSO (dimethyl sulfoxide).
The optical density was measured at 570nm using multi-well reader and the results were expressed as percent viability. Since the positive control (DMEM with 10% FBS) represented 100% viability, the treated cells were calculated as a percentage of the control. The analysis was performed in six replicates (n=6).

2.3.2. Endothelial cell migration Assay

To evaluate the pro-migratory potential of the products released by the different kinds of aerogels, a cell migration assay (scratch test) was conducted. For this purpose, early in the morning 70 000 primary human endothelial cells (GFP+-HUVEC) were seeded in 96-well plates (Imagelock, Sartorius, Germany) within 100 µL of EGM-2 cell culture medium (Endothelial Cell Growth Basal Medium-2, Lonza). This seeding density allows to obtain a confluent monolayer when cells adhere. To obtain calibrated scratch (750µm width) in each well of 96-well plate, Wound Maker device (Sartorius, Germany) was used on the evening of the seeding day. Supernatants were immediately removed to discard floating wounded cells. Cells were then incubated with 100µl of conditioned media or control media (non-conditioned). The conditioned media were prepared by incubating the aerogels in complete EGM-2 for 24h at 37°C. The volume of medium per aerogel and the incubation period (24h) were similar as for the MTT assay described above. Then, plates were placed in Videomicroscope Incucyte® S3 (Sartorius, Germany), equipped with scratch wound analysis module. Wound closure was monitored by taking 10X pictures every hour for 24h. Pictures were analysed using the Incucyte S3 associated software. Results are expressed as wound density, meaning cell confluence measurement within the initial margins of the wound. The analysis was performed in six replicates (n=6).

2.3.3. Cell Proliferation measurement

BALB-3T3 fibroblasts cells were seeded onto hPL gels at a population density of 200000 cells in 2 mL and cell proliferation was analyzed on days 1,7,10,20 and 30. At each time point, the metabolic activity of viable and attached cells was determined by Alamar blue assay (Alamar blue kit, Invitrogen). Briefly, after each incubation time, the culture medium was discarded, the samples were washed twice with Dulbecco's phosphate-buffered saline solution (DPBS,Gibco, New York, USA,) and transferred to a new 24 well plate. Then, 1 mL of complete DMEM supplemented with 10% FBS and 5% resazurin solution were added to each well, and the cells were incubated for 2 hours with 5% CO_2, at 37°C. The supernatants were transferred to a black 96-well plate, and the fluorescence was read with an excitation wavelength at 560 nm and an emission wavelength at 590 nm with a microplate reader. The analysis was performed in four replicates (n=4).

 doi:10.20944/preprints202401.0132.v1

2.3.4. Cell morphology

The cell morphology was evaluated by scanning electron microscopy according to a method previously described [30]. It consists of rinsing the samples with a 0.125 mM cacodylate solution and fixing them with 4%glutaraldehyde in 50 mM cacodylate buffer (Thermo Scientific Chemicals) for 2.5 hours at room temperature. Dehydration in a gradient of ethanol and then treated with HDMS for 30 min.

The samples were then coated with a 6nm platinum layer using a sputtering machine (SI50B Sputter Coater -Edwards, UK) and observed using scanning electron microscopy (Quanta 250 FEG FEI, Thermo Scientific, USA). All observations were made in the secondary electron emission mode with high voltage of 5 kV. The analysis was performed in four replicates (n=4).

2.4. Statistical analysis :

The experiments were conducted a minimum of three times, and the results are presented as mean ± standard deviation (SD). Statistical analyses were performed using GraphPad Prism 8 software (GraphPad Software, Inc., La Jolla, CA, USA). To assess differences between groups, an unpaired t-test with Welch's correction was employed, with statistical significance set at $p < 0.05$. Additionally, ordinary one-way analysis of variance (ANOVA) was conducted, followed by Dunnett's multiple comparisons test, with a significance threshold of $p < 0.05$. These specific statistical tests were chosen to rigorously evaluate the obtained data and identify significant differences among experimental group.

3. Results and Discussion

3.1. hPL aerogels conception

hPL, rich in bioactive molecules, including coagulation factors such as fibrinogen, thrombin, and factor XII, serves as a foundation for developing our hydrogels. The incorporation of calcium ions via $CaCl_2$ addition initiates a three-dimensional fibrin network formation within the hydrogels [31].

As water is immiscible with $scCO_2$, before proceeding with supercritical CO_2 drying, an essential step involves substituting the initially present water with acetone. To ensure structural integrity, we gradually increased the acetone concentration in incremental steps of 25% (v/v) during the substitution process [32]. Final immersion in 100% acetone was repeated to guarantee complete solvent exchange.

Supercritical CO_2 drying allows for the production of dry hPL aerogels. The obtained aerogels exhibited stable shape, and their dimensions were similar to those of the hydrogels, indicating no major structural collapse. This preservation of structure was macroscopically observed and depicted in Figure 1.

Scanning electron microscopy (SEM) images were utilized to compare the three-dimensional network structure between the hydrogel and aerogel obtained after $scCO_2$ drying. The results of this analysis, presented in Figure 2 (B,D), demonstrate the preservation of the three-dimensional fibrin network. The network fibers exhibited a rough, non-smooth appearance compared to purified fibrin fibres [33]. This roughness is potentially attributed to other hPL components, especially, proteins that attach to the network. Previous studies have shown that certain growth factors such as β-FGF and VEGF have an affinity for fibrin network [34].

Preprints (www.preprints.org) | NOT PEER-REVIEWED | Posted: 3 January 2024 doi:10.20944/preprints202401.0132.v1

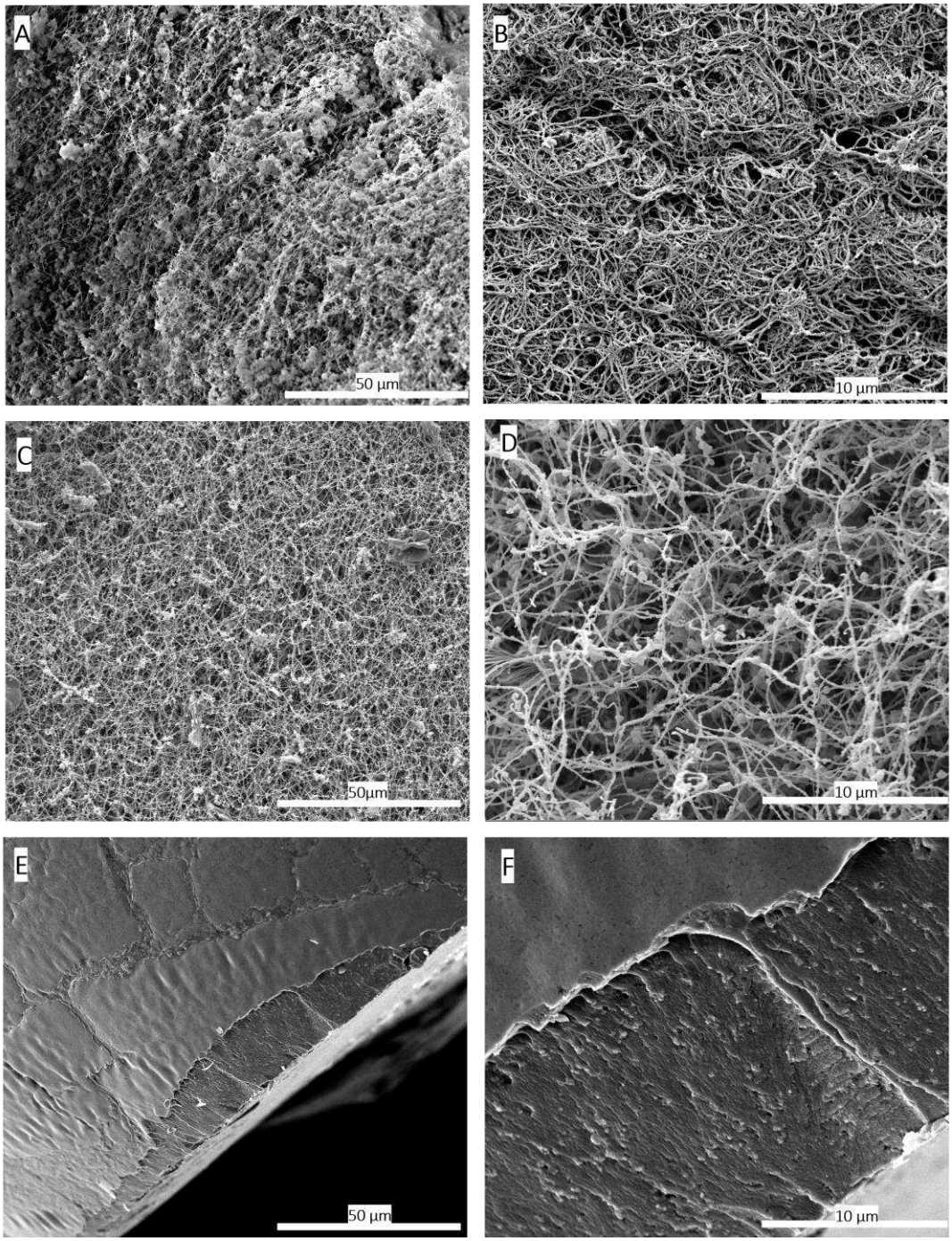

Figure 2. Scanning electron microscopy (SEM) images comparing the 3D structure of fibrin networks in platelet lysate hydrogels (A, B) and aerogels (C, D), along with hydrogels dried conventionally in an oven at 37°C (E, F). (A) SEM image of the hydrogel at a magnification of 1000x, (B) SEM image of the hydrogel at a magnification of 5000x, illustrating the formed fibrin network. (C) SEM image of the hPL aerogel at 1000x magnification, (D) SEM image of the hPL aerogel at 5000x magnification, confirming the preservation of the fibrin network's structural integrity through the supercritical CO_2-based shaping process. (E) SEM image of the hydrogel dried in an oven at 37°C at a magnification of 1000x, and (F) SEM images of hydrogels dried in an oven at 37°C at a magnification of 5000x. These images highlight the adverse effects of conventional drying on the three-dimensional fibrin network structure, resulting in a flattened and non-porous fibrin structure. These findings provide conclusive evidence of the destructive impact of oven drying at 37°C on the three-dimensional fibrin network, resulting in a flattened and non-porous structure.

 doi:10.20944/preprints202401.0132.v1

$ScCO_2$ drying is considered the gentlest method for shaping aerogels, as it prevents shrinkage or collapse of three-dimensional network of gels [35]. In contrast, conventional drying methods at room temperature or in ovens can cause structural collapse due to capillary forces [36]. This is clearly evident when comparing SEM images of hPL hydrogels dried in an oven at 37°C to hPL aerogels obtained through $scCO_2$ drying. In the case of aerogels, the three-dimensional fibrin network structure is preserved, whereas the hydrogel dried in the oven exhibits complete collapse of the three-dimensional network and pore shrinkage as presented in figure 2 (E,F) due to capillary forces [37]. The SEM observations are confirmed by the porosity measurements carried out by the mercury porosimeter on the 2 types of materials (Table 1).

According to the International Union of Pure and Applied Chemistry (IUPAC), aerogels are officially defined as "microporous solids in which the dispersed phase is a gas" [38]. These materials are renowned for their exceptional properties, characterized by ultra-low density (approximately 0.003 to 0.5 g/cm^3), high porosity (80% to 99.8%), high specific surface area (500 to 1200 m^2/g), and ultralightweight [39]. Remarkably, our fabricated aerogels exhibit exceptional porosity, averaging at approximately 93.9% (Table 1), and display a consistent density of approximately 0.09806 cm^3/g, aligning closely with the defining characteristics of aerogels as established by IUPAC.

Table 1. Comparison of Porosity Measurements between hPL hydrogels and Aerogels. Porosity measurements obtained through mercury porosimetry for both hPL hydrogels and aerogels, providing quantitative data to support SEM observations.

	Aerogel dried using $scCO_2$	**Hydrogel oven dried at 37°C**
otal porosity between 4 nm and 360 μm (%)	93,9 % ± 2 %	7,9 % ± 4 %

3.2. Mechanical propreties comparaison

The Texture profile analysis (TPA) test conducted on hPL hydrogels and hPL aerogels allowed for the determination of their mechanical properties and a comparison of their strength. Hardness and adhesiveness parameters were measured and compared (figure 3).

Hardness represents the maximum force required to compress the sample and is calculated from the peak force during the first compression cycle. Adhesiveness measures the ability of a material to stick or adhere to the contact surface with the piston and is calculated by determining the negative area between the two compression cycles [40]. The results demonstrated that aerogels exhibit significantly higher hardness compared to hydrogels and are less adhesive. This greatly enhances their manipulability, as depicted in Figure 3 (C,D).

Platelet lysate hydrogels contain a significant amount of water, which imparts flexibility and low mechanical rigidity, making them easily deformable and limiting their handling. In contrast, aerogels are more rigid due to their three-dimensional porous structure, providing them with higher rigidity. Additionally, the absence of water significantly reduces adhesiveness, making them easy to handle and suitable for applications requiring structural stability. The developed aerogels exhibit much higher mechanical stability compared to hydrogels. They can maintain their structure for several months, unlike hydrogels, which experience complete structural collapse within a few hours due to capillary forces.

Preprints (www.preprints.org) | NOT PEER-REVIEWED | Posted: 3 January 2024 doi:10.20944/preprints202401.0132.v1

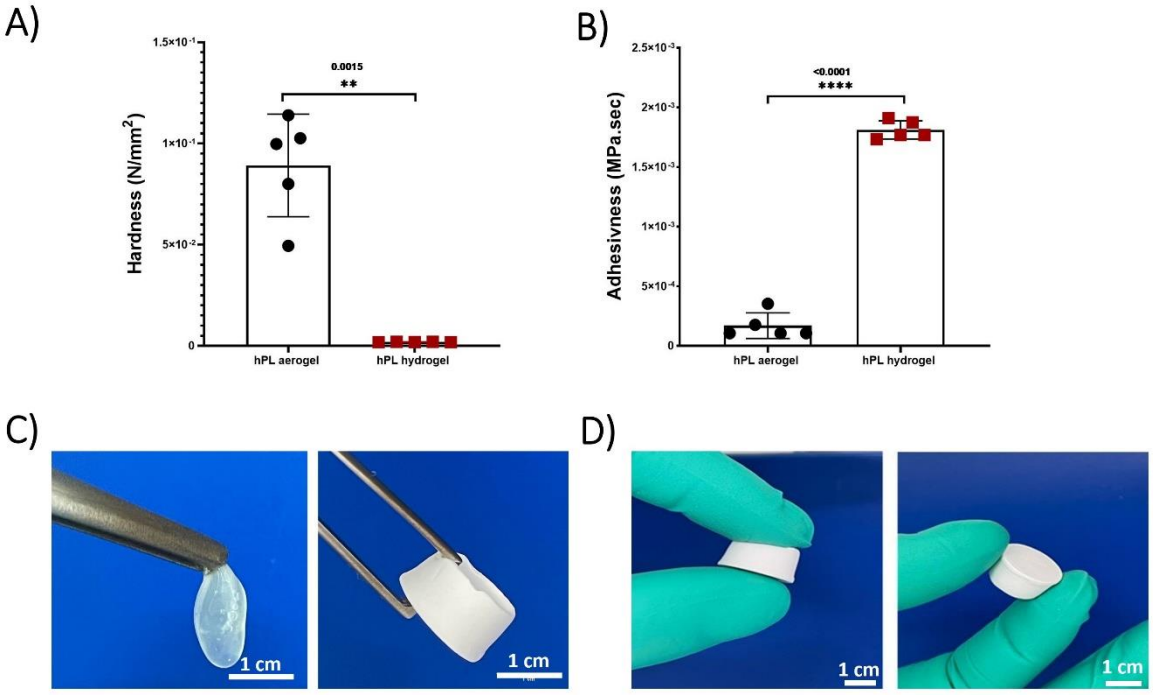

Figure 3. (A) Hardness measurements comparing hydrogels and aerogels. (B) Adhesiveness measurements between hydrogels and aerogels. (C) Macroscopic mechanical properties of hydrogels and aerogels. (D) Aerogel manipulability. Data represent the mean of 5 replicates, and statistical significance was assessed using Unpaired t-test with Welch's correction for $p < 0.05$ (**$p < 0.01$, ****$p < 0.0001$).

3.3. Hydrophobic-hydrophilic characteristics and absorption properties of hPL Aerogels.

The absorption properties of aerogels are of great interest due to their ability, once implanted, to interact with surrounding fluids, facilitating the integration of vital components and key players in the tissue regeneration process, such as growth factors and cells.

When placed in PBS, hPL aerogels exhibit a remarkable capacity for rapid fluid absorption. Within approximately 120 minutes, these aerogels attain a steady state in their swelling behavior as illustrated in Figure 4 (A). Consequently, in this relatively short period, the material absorbs an impressive 87% of its own weight in PBS as shown in Figure 4 (B). Notably, while achieving this rapid absorption rate, the structural integrity of the samples remains unaffected, and upon rehydration, they regain an appearance akin to that of the hydrogel before drying "data not show".

Contact angle studies were conducted to analyse the hydrophobicity and hydrophilicity properties of the surface. Immediately after the deposition of the PBS droplet, an initial average contact angle of approximately 115 degrees was observed in the first few seconds, indicating a hydrophobic behaviour. The contact angle rapidly decreased until reaching 0 degrees after 25 seconds, indicating a hydrophilic behaviour Figure 4 (C,D). This rapid absorption suggests a highly interesting haemostatic property which is crucial for wound healing process[41].

Preprints (www.preprints.org) | NOT PEER-REVIEWED | Posted: 3 January 2024 doi:10.20944/preprints202401.0132.v1

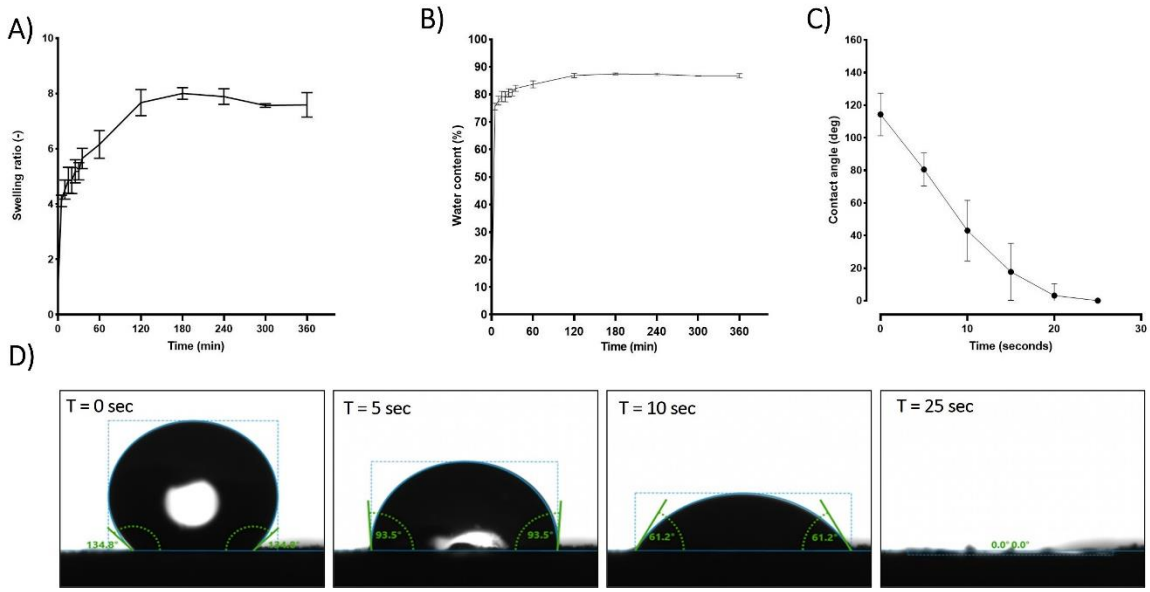

Figure 4. Comprehensive analysis of hPL aerogel behaviour in contact with liquid (PBS), including: (A) the swelling ratio, (B) water content, (C) contact angle, and (D) visual representation of droplet interaction. These results contribute to understanding the dynamic response and surface properties of hPL aerogels in a liquid environment. Error bars represent standard deviation (n=3).

Platelet lysate is composed of a variety of biological compounds with distinct hydrophilic/hydrophobic characteristics. The initially observed hydrophobicity in contact angle measurements can be attributed to surface ionic interactions between lipids, glycoproteins, and the formed fibrin network, resulting in a coating that imparts hydrophobic character to the surface [42]. Although this hydrophobicity is present initially, it does not hinder the rapid and significant absorption of the fluids (within seconds), which is associated with an appropriate hydrophilicity for this type of material. In addition to being influenced by the fabricated porous nature, the hydrophobicity of aerogels also depends on the other hydrophilic constituents present. Proteins, which are an essential part of platelet lysate, are composed of amino acids. Each amino acid possesses its own characteristics in terms of polarity and charge, and thus its own hydrophilicity/hydrophobicity, which explains the coexistence of both phenomena.

3.4. Chemical strcture analysis (FTIR)

FTIR-ATR (Attenuated Total Reflectance) spectroscopy was used to obtain spectra of hPL aerogels and liquid hPL (Figure 5). Characteristic peaks of amide I (1633 cm-1/1634 cm-1) correspond to C=O stretching, amide II (1546 cm-1/1537 cm-1) correspond to N-H bending and C-N stretching bands, and amide III (1243 cm-1/1242 cm-1). Peaks around 1397 cm-1/1393 cm-1 are characteristic of platelet lysate [42] and are attributed to its different constituents. This indicates that the chemical structure is potentially unaffected by the $scCO_2$ drying process and potentially preserved.

In the case of aerogels, a decrease is observed in the amide A band, which corresponds to the peak at around 3277 nm, and an increase in the peaks of amide I and amide II. This suggests that the amount of -NH2 groups available in the proteins decreased and mostly like it was converted into C-N (amide II). This can be explained by protein-protein interactions such as fibrin network formation (fibrinogen polymerization) and interactions between other proteins in the platelet lysate, either with each other or with the formed fibrin network [43].

Preprints (www.preprints.org) | NOT PEER-REVIEWED | Posted: 3 January 2024 doi:10.20944/preprints202401.0132.v1

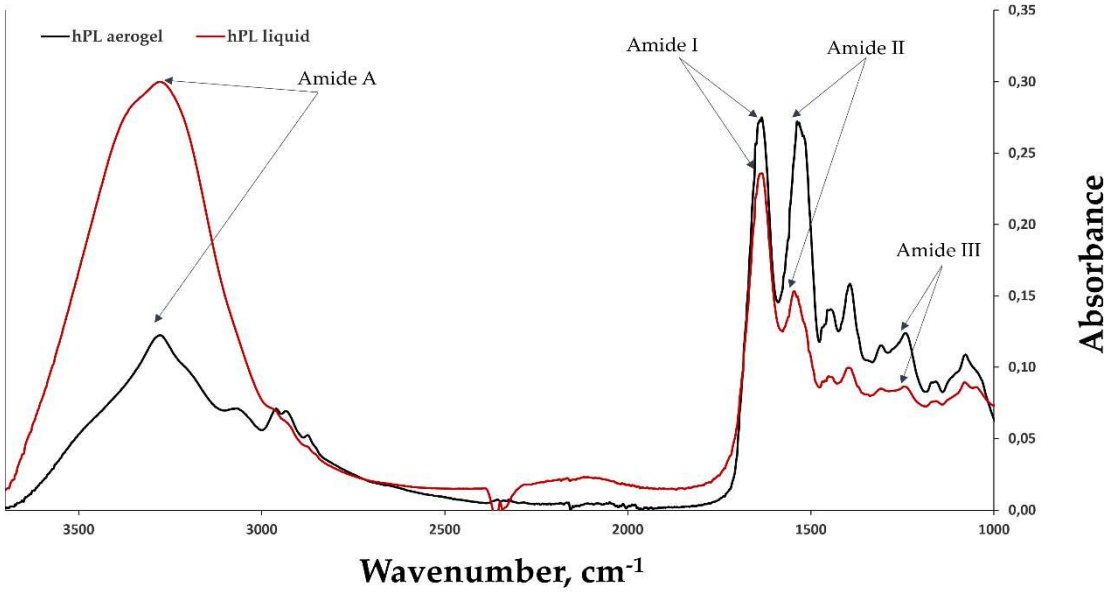

Figure 5. The FTIR spectra of liquid hPL (in red) and hPL aerogels (in black), highlighting the characteristic peaks of amides I, II, III, and A. The comparison between the FTIR spectra of liquid hPL and hPL aerogels allows for the assessment of any structural changes or preservation of molecular characteristics induced by the aerogel formation process. The results provide valuable insights into the chemical composition and structural integrity of hPL aerogels.

3.5. Release kinetics of total proteins and VEGF from hPL aerogels.

The cumulative release of total proteins is depicted in Figure 6(A), illustrating the release profiles of proteins from both aerogels and hydrogels over time. Notably, the protein release profile from aerogels exhibited a sustained release pattern compared to hydrogels throughout the entire duration of testing. Specifically, hydrogels released 50% of the total proteins within 23 hours, while aerogels extended this release to 44 hours

However, both release profiles exhibited a typical sustained release pattern which begins with: i) rapid and high initial protein release during the first 4 hours, potentially due to freely unbound proteins that can be easily removed from sample surfaces. ; ii) a phase during which the free proteins contained inside the material are released by diffusion within the porous network (between 24 and 72 hours); iii) and finally, a slower and prolonged release of up to 168 hours which may be associated with the progressive degradation of the material. The release of total proteins therefore depends on several factors, such as the size of the sample and in particular its external surface, area in contact with the liquid (first phase of release), the porosity of the material (second phase of release) and the speed of degradation of the network of fibrin (third phase of release).

Thus, the total proteins present in aerogels have a slower release speed than that observed for hydrogels due in part to the time necessary to hydrate the aerogel, deploy the fibrin fibers and reduce the strength of the bonds created during the condensation of the growth factors on the fibrous networks.

Even though the cumulative percentage of total protein release occurs more gradually in the aerogels which is relevant for clinical applications, it is important to note that the results obtained from protein quantification showed significantly lower protein content in the aerogels at 168 hours (Figure 6 B). This could be attributed to a potential protein loss during the shaping process such as the acetone baths or rinsing with liquid CO_2 [44].

Platelet lysate is a rich source of growth factors and cytokines that play an effective role in wound healing and the recruitment of cells involved in tissues repair [45]. Among the many growth factors contained in platelet lysate, it has been shown that VEGF release plays a crucial role in angiogenesis, contributing to the formation of new blood vessels, restoring vascularization, and

Preprints (www.preprints.org) | NOT PEER-REVIEWED | Posted: 3 January 2024 doi:10.20944/preprints202401.0132.v1

supporting tissue repair. It has also been demonstrated that VEGF is involved in cell recruitment and can increase vascular permeability, facilitating the passage and migration of immune blood cells that participate in the inflammatory response and healing process [46].

To confirm that the growth factors are still in aerogels, a release kinetics study of VEGF was conducted using an ELISA test (Figure 6 C). The kinetic profile of VEGF release exhibited a sustained pattern similar to that observed for the total protein release. By comparing the concentration of released VEGF from aerogels to that of liquid platelet lysate, no significant difference was observed, indicating that there is no significant loss of VEGF during the shaping process. This can be attributed to the affinity between VEGF and the fibrin network [47].

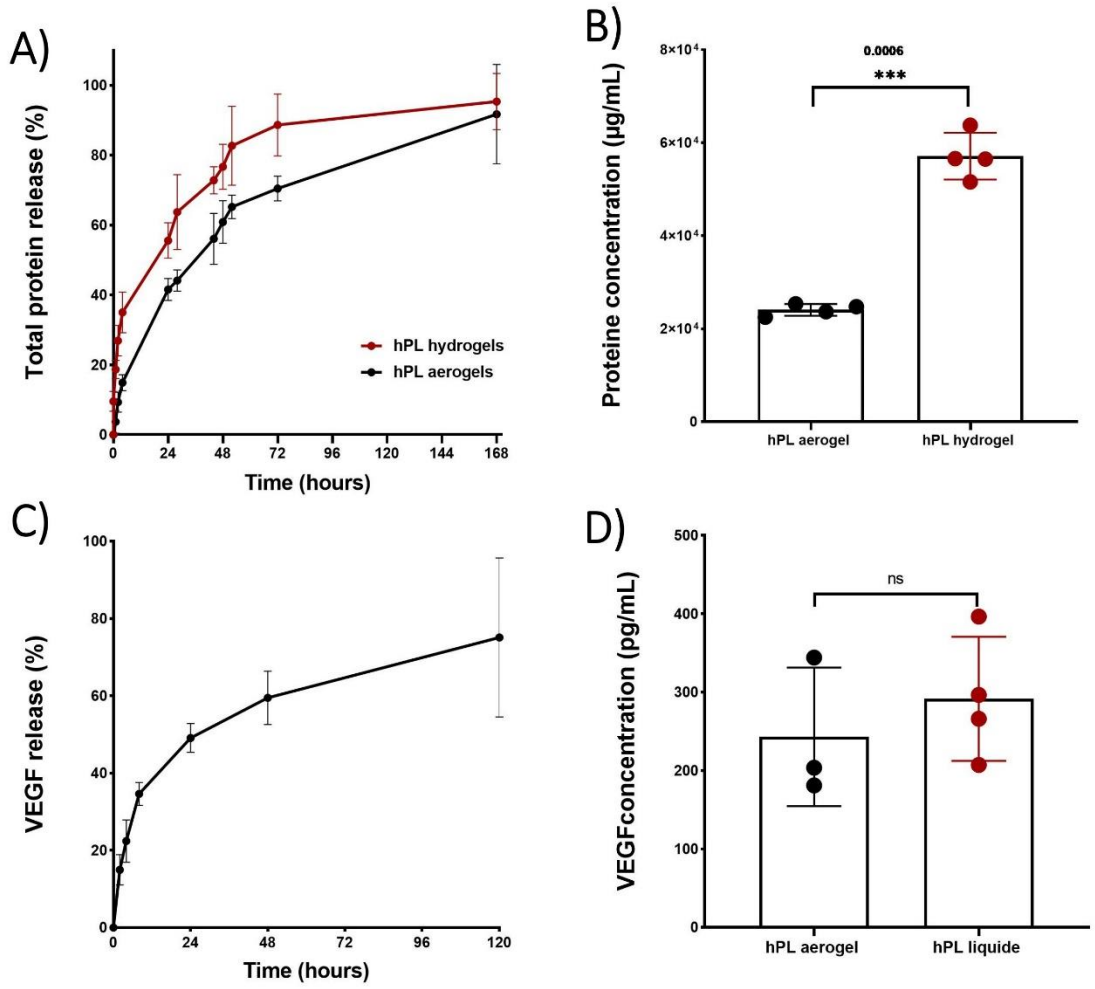

Figure 6. Results of release studies, quantifying total protein release and VEGF release. (A) Comparison of release kinetics, presented as percentages, between hPL aerogels (in black) and hPL hydrogels (in red). (B) Comparison of released protein concentrations between hPL aerogels and hPL hydrogels at 168 hours. (C) Release kinetics of VEGF from hPL aerogels and hPL liquid. (D) Comparison of VEGF concentrations in hPL aerogels at 120 hours and liquid hPL. Statistical significance assessed via Unpaired t test with Welch's correction for $p<0.05$ (**$p < 0.01$, ns > 0.05). Error bars represent standard deviation (n=3).".

3.6. Efficacy assessment of hPL aerogels released Products: Metabolic Activity and Cell Migration Analysis

The assessment of the effect of the products released by the aerogels (growth factors, cytokines, degradation products, etc.) is carried out using a MTT assay based on the recommended indirect method described in ISO 10993-5 standard [48]. The results obtained are presented in the Figure 7 (A). BALB-3T3 cells cultured with the conditioned medium from freshly prepared aerogels (New hPL

 doi:10.20944/preprints202401.0132.v1

aerogels extract) showed a high percentage of metabolic activity (92.45%) with no significant difference to cells treated with standard culture medium containing 10% FBS (considered as 100%). Contrastingly, cells treated with DMEM alone exhibited significantly reduced metabolic activity (45.11%) (p-value <0.0001). This finding indicates that the products released from the aerogels retain their functionality and are capable of eliciting a biological response by enhancing cellular metabolic activity of BALB-3T3 cells.

To assess the long-term stability of the aerogels, we examined samples that were prepared 24 months prior and stored in the dark at room temperature (Old hPL aerogels extract). These samples demonstrated nearly equivalent metabolic activity (89.91%) when compared to the freshly prepared aerogels, suggesting that the aerogels maintain their biological efficacy over time when stored appropriately.

These results are consistent with results previously obtained by Andia et al. who showed that platelet derivatives such as such as PRP and hPL in dry form preserve the effectiveness of their bioactive molecules (growth factors, cytokines, etc.) for a duration that can extend to several months [49]. Some even consider lyophilization as an optimal storage method for hPL [50].

Thus, these two drying processes (freeze-drying and drying in supercritical CO_2) by eliminating water from the aerogels make it possible to avoid the degradation of proteins and other biological compounds present in hPL [51]. Additionally, the removal of water significantly reduces enzymatic oxidation reactions and bacterial growth, contributing to increased stability of the platelet lysate.

Endothelial cell migration is an important mechanism that contributes to tissue formation and is essential for wound healing and tissue regeneration [52].

The results of cellular migration tests conducted on endothelial cells (GFP+-HUVEC) are presented in Figure 7 (B,C). After 24 hours, the cells treated with conditioned media were significantly more confluent at the scratch site compared to cells treated with the control (p-value 0.0467).

Platelet lysate is rich in factors that promote the migration of endothelial cells, such as PDGF and VEGF. ELISA test confirmed that the aerogels contained and could release VEGF. These results suggest that hPL aerogels contain and release functional pro-angiogenic factors that can promote the migration of endothelial cells.

The results demonstrate that the growth factors originally present in the liquid platelet lysate, or at least a portion of them, are still present and can promote the migration of endothelial cells hen released.

Preprints (www.preprints.org) | NOT PEER-REVIEWED | Posted: 3 January 2024 doi:10.20944/preprints202401.0132.v1

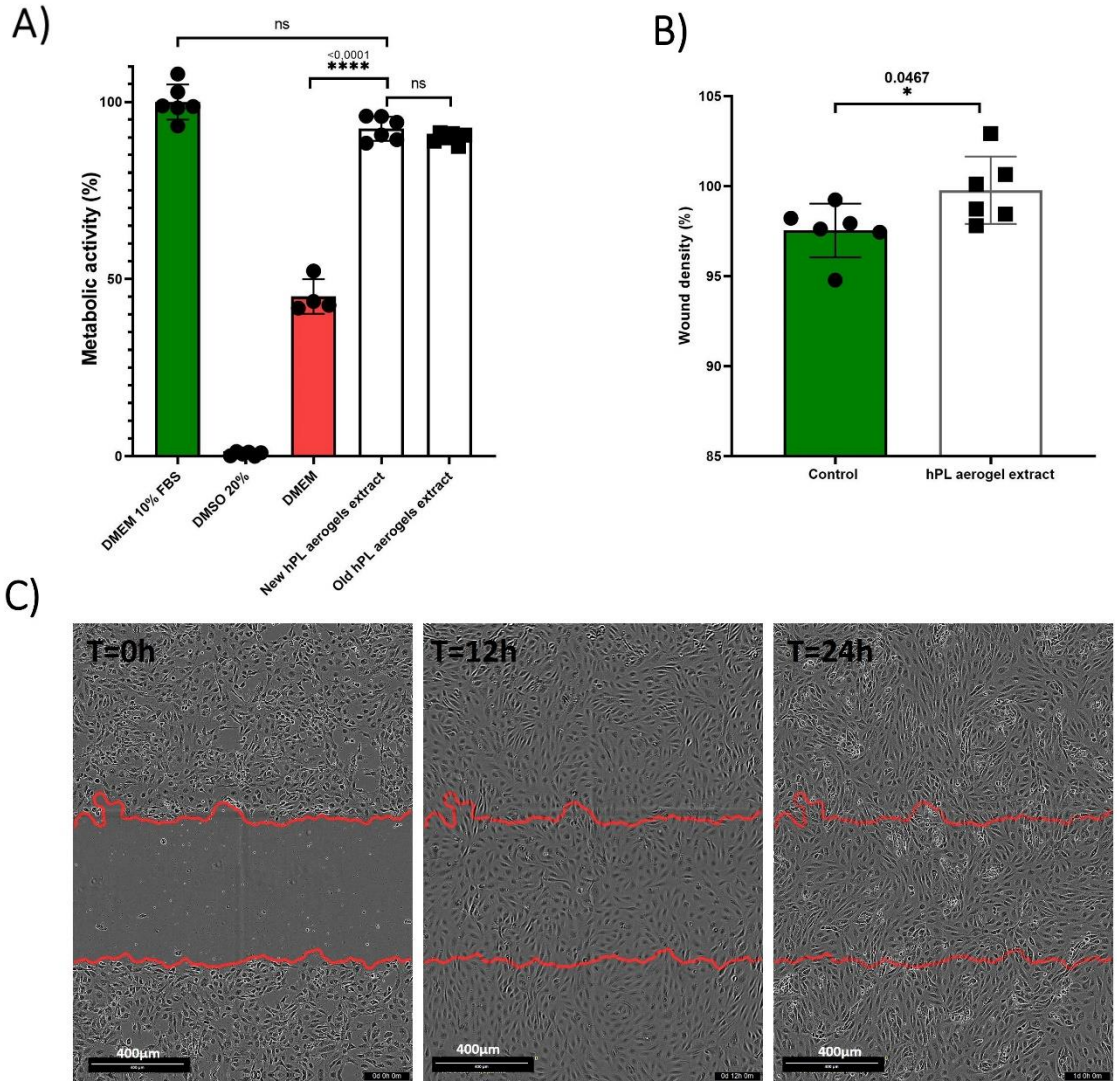

Figure 7. This figure presents the results of the biological evaluation of products released by hPL aerogels. (A) The graph represents the metabolic activity of BALB 3T3 cells when exposed to the media conditioned by hPL aerogels, as measured by the MTT assay. Error bars represent standard deviation. (B) The graph displays the results of the scratch assay performed on HUVEC cells. It illustrates the migration capability of HUVEC cells when exposed to the released products from hPL aerogels. Error bars represent standard deviation. (C) The images show the scratch assay at T=0h , T=12h and T=24h, providing a visual representation of cell migration in response to the released products. The statistical significance of the results was studied using Ordinary one-way ANOVA and unpaired t test with Welch's correction for $p<0.05$ (*$p < 0.05$, ns > 0.05). Error bars represent standard deviation (n=6).

3.8. Cell Adhesion and Proliferation on Platelet Lysate Aerogels

The in-vitro analysis of adhesion and proliferation of BALB-3T3 cells seeded on platelet lysate aerogels was evaluated through the measurement of metabolic activity using Alamar Blue assay. The results graphically presented in Figure 8(A) clearly demonstrate a significant increase in signal over the course of days, correlating with an increase in metabolic activity and cell number [53]. These results indicate that around 70% of the seeded cells adhere, adapt, and proliferate, suggesting that the three-dimensional fibrin network forming the aerogel maintains its biocompatibility and can be used as a cell culture support. The fibrin network can be considered a supportive substrate for cell adhesion and proliferation [54]. The drying process allows the formation of aerogels that preserve this characteristic, as evidenced by scanning electron microscopy (SEM) images of the seeded cells.

Preprints (www.preprints.org) | NOT PEER-REVIEWED | Posted: 3 January 2024 doi:10.20944/preprints202401.0132.v1

At Day 1, the cells start to adhere to the network, and over the course of days, an increase in cell density is observed at Day 7 and Day 30 (Figure 8 B).

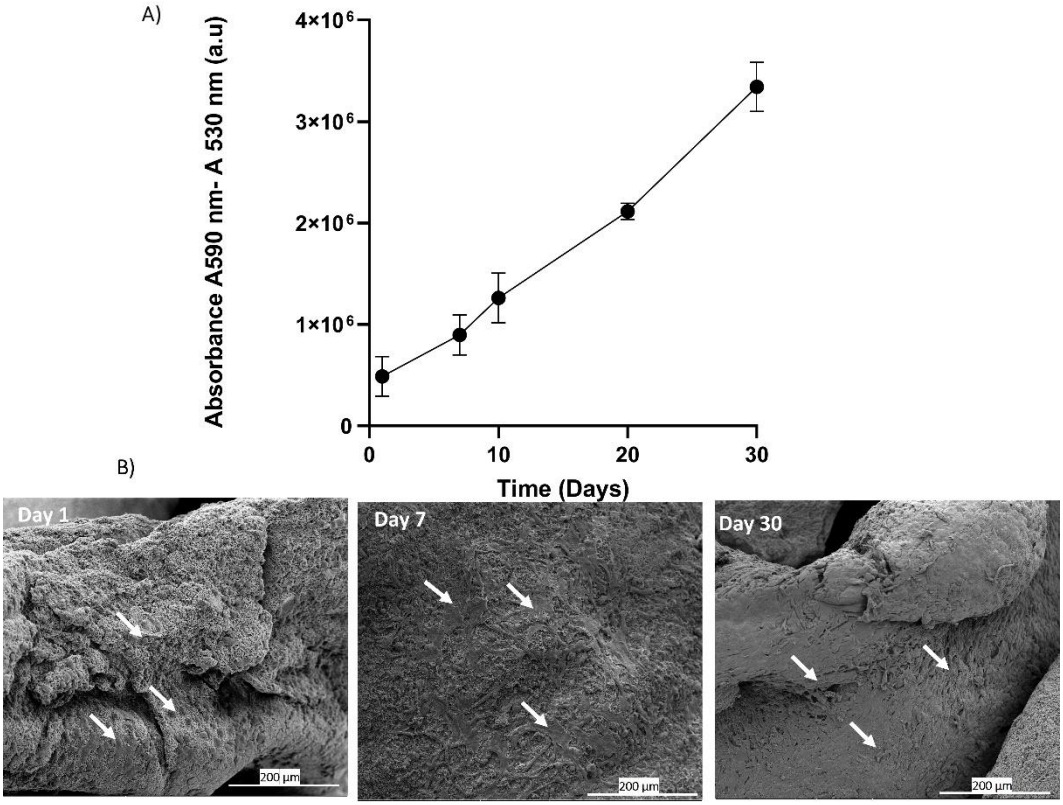

Figure 8. This figure presents the results of cell seeding directly onto hPL aerogels. (A) The graph shows the measurement of metabolic activity using the Alamar Blue assay at days 1, 7, 10, 20, and 30. It indicates the viability and metabolic activity of Balb-3T3 cells cultured on hPL aerogels over time. (B) The images display scanning electron microscopy (SEM) images of cells deposited on the hPL aerogels at day 1, day 7, and day 30.

4. Conclusions

Hemoderivative products such as platelet lysate are widely used in tissue engineering due to their rich source of growth factors that promote tissue repair and regeneration. However, their use in the form of hydrogels is severely limited as this form significantly hampers their manipulability and stability, not to mention the challenge of ensuring sustained release over time. The aerogels developed in this study have mechanical properties suitable for tissue engineering applications and in particular for good handling and most importantly, long-term structural stability, which is uncommon for platelet lysate-based biomaterials.

Scaffolds/biomaterials require properties such as biocompatibility, appropriate microstructure, mechanical strength, and the ability to support cell residence while releasing bioactive molecules such as VEGF that remain effective and can fulfil their functions. The obtained results demonstrate that the LP aerogels developed through supercritical CO_2 drying perfectly meet these characteristics, making them preferred biomaterials for tissue engineering while serving as an autologous source of bioactive molecules. Indeed, they possess a combination of properties that promote tissue repair as they are more stable, capable of releasing active biomolecules (growth factors, cytokines, etc.), and support cell adhesion and proliferation.

5. Patents

PLATELET LYSATE FOAM FOR CELL CULTURE, CELL THERAPY AND TISSULAR REGENERATION AND METHOD FOR OBATINING SAME. Publication number: 20230119928

Author Contributions: For research articles with several authors, a short paragraph specifying their individual contributions **must be provided**. The following statements should be used "Conceptualization, **SC,**and **TC**.; methodology, **FT,AM and CM**; software, **FT**.; validation, **SC ADB ,PL, LG,LP**, and **MR** ; formal analysis, **FT DG**.; investigation, **FT** .; resources, **SC, ADP , PL, and LP** .; data curation, **FT** and **SC** .; writing—original draft preparation **FT**.; writing—review and editing FT, SC, ADB, PL, LG, LP and AM .; visualization, **FT**.; supervision, **SC** and **ADB**.; project administration, **SC** and **ADB**.; funding acquisition, , **SC** and **ADB**.

Data Availability Statement: Data from this article are available upon reasonable request.

Acknowledgments: The authors would like to thank the Head and Neck Cancer Organ Committee of the Institut Universitaire du Cancer de Toulouse Oncopole for funding equipment and travel expenses. We would like to thank the Institut de Chimie de Toulouse ICT – UAR 2599 (Université de Toulouse, CNRS, Toulouse, France – www.ict.cnrs.fr) for its participation in the purchase of the videomicroscope used in this study.

Conflicts of Interest: The authors declare no conflict of interest. And the funders had no role in the design of the study; in the collection, analyses, or interpretation of data; in the writing of the manuscript; or in the decision to publish the results".

References

1. Holinstat, M. Normal Platelet Function. *Cancer and Metastasis Reviews* 2017, *36*, 195–198.
2. Tomaiuolo, M.; Brass, L.F.; Stalker, T.J. Regulation of Platelet Activation and Coagulation and Its Role in Vascular Injury and Arterial Thrombosis. *Interv Cardiol Clin* 2017, *6*, 1–12.
3. van der Meijden, P.E.J.; Heemskerk, J.W.M. Platelet Biology and Functions: New Concepts and Clinical Perspectives. *Nat Rev Cardiol* 2019, *16*, 166–179.
4. De Pascale, M.R.; Sommese, L.; Casamassimi, A.; Napoli, C. Platelet Derivatives in Regenerative Medicine: An Update. *Transfus Med Rev* 2015, *29*, 52–61.
5. Burnouf, T.; Strunk, D.; Koh, M.B.C.; Schallmoser, K. Human Platelet Lysate: Replacing Fetal Bovine Serum as a Gold Standard for Human Cell Propagation? *Biomaterials* **2016**, *76*, 371–387, doi:10.1016/j.biomaterials.2015.10.065.
6. Zamani, M.; Yaghoubi, Y.; Movassaghpour, A.; Shakouri, K.; Mehdizadeh, A.; Pishgahi, A.; Yousefi, M. Novel Therapeutic Approaches in Utilizing Platelet Lysate in Regenerative Medicine: Are We Ready for Clinical Use? *J Cell Physiol* **2019**, *234*, 17172–17186, doi:10.1002/jcp.28496.
7. Phipps, M.C.; Xu, Y.; Bellis, S.L. Delivery of Platelet-Derived Growth Factor as a Chemotactic Factor for Mesenchymal Stem Cells by Bone-Mimetic Electrospun Scaffolds. *PLoS One* **2012**, *7*, doi:10.1371/journal.pone.0040831.
8. Kurita, J.; Miyamoto, M.; Ishii, Y.; Aoyama, J.; Takagi, G.; Naito, Z.; Tabata, Y.; Ochi, M.; Shimizu, K. Enhanced Vascularization by Controlled Release of Platelet-Rich Plasma Impregnated in Biodegradable Gelatin Hydrogel. *Annals of Thoracic Surgery* **2011**, *92*, 837–844, doi:10.1016/j.athoracsur.2011.04.084.
9. Schallmoser, K.; Bartmann, C.; Rohde, E.; Reinisch, A.; Kashofer, K.; Stadelmeyer, E.; Drexler, C.; Lanzer, G.; Linkesch, W.; Strunk, D. Human Platelet Lysate Can Replace Fetal Bovine Serum for Clinical-Scale Expansion of Functional Mesenchymal Stromal Cells. *Transfusion (Paris)* **2007**, *47*, 1436–1446, doi:10.1111/j.1537-2995.2007.01220.x.
10. Chevallier, N.; Anagnostou, F.; Zilber, S.; Bodivit, G.; Maurin, S.; Barrault, A.; Bierling, P.; Hernigou, P.; Layrolle, P.; Rouard, H. Osteoblastic Differentiation of Human Mesenchymal Stem Cells with Platelet Lysate. *Biomaterials* **2010**, *31*, 270–278, doi:10.1016/j.biomaterials.2009.09.043.
11. Markazi, R.; Soltani-Zangbar, M.S.; Zamani, M.; Eghbal-Fard, S.; Motavalli, R.; Kamrani, A.; Dolati, S.; Ahmadi, M.; Aghebati-Maleki, L.; Mehdizadeh, A.; et al. Platelet Lysate and Tendon Healing: Comparative Analysis of Autologous Frozen-Thawed PRP and Ketorolac Tromethamine in the Treatment of Patients with Rotator Cuff Tendinopathy. *Growth Factors* **2022**, *40*, 163–174, doi:10.1080/08977194.2022.2093198.
12. Shanbhag, S.; Mohamed-Ahmed, S.; Lunde, T.H.F.; Suliman, S.; Bolstad, A.I.; Hervig, T.; Mustafa, K. Influence of Platelet Storage Time on Human Platelet Lysates and Platelet Lysate-Expanded Mesenchymal Stromal Cells for Bone Tissue Engineering. *Stem Cell Res Ther* **2020**, *11*, doi:10.1186/s13287-020-01863-9.
13. De Angelis, E.; Grolli, S.; Saleri, R.; Conti, V.; Andrani, M.; Berardi, M.; Cavalli, V.; Passeri, B.; Ravanetti, F.; Borghetti, P. Platelet Lysate Reduces the Chondrocyte Dedifferentiation during in Vitro Expansion: Implications for Cartilage Tissue Engineering. *Res Vet Sci* **2020**, *133*, 98–105, doi:10.1016/j.rvsc.2020.08.017.
14. Li, T.; Lu, H.; Zhou, L.; Jia, M.; Zhang, L.; Wu, H.; Shan, L. Growth Factors-Based Platelet Lysate Rejuvenates Skin against Ageing through NF-KB Signalling Pathway: In Vitro and in Vivo Mechanistic and Clinical Studies. *Cell Prolif* **2022**, *55*, doi:10.1111/cpr.13212.
15. da Fonseca, L.; Santos, G.S.; Huber, S.C.; Setti, T.M.; Setti, T.; Lana, J.F. Human Platelet Lysate – A Potent (and Overlooked) Orthobiologic. *J Clin Orthop Trauma* 2021, *21*.

16. Meftahpour, V.; Malekghasemi, S.; Baghbanzadeh, A.; Aghebati-Maleki, A.; Pourakbari, R.; Fotouhi, A.; Aghebati-Maleki, L. Platelet Lysate: A Promising Candidate in Regenerative Medicine. *Regenerative Med* 2021, *16*, 71–85.
17. Costa-Almeida, R.; Calejo, I.; Altieri, R.; Domingues, R.M.A.; Giordano, E.; Reis, R.L.; Gomes, M.E. Exploring Platelet Lysate Hydrogel-Coated Suture Threads as Biofunctional Composite Living Fibers for Cell Delivery in Tissue Repair. *Biomedical Materials (Bristol)* **2019**, *14*, doi:10.1088/1748-605X/ab0de6.
18. Alhawari, H.; Jafar, H.; Al Soudi, M.; Ameereh, L.A.; Fawaris, M.; Saleh, M.; Aladwan, S.; Younes, N.; Awidi, A. Perilesional Injections of Human Platelet Lysate versus Platelet Poor Plasma for the Treatment of Diabetic Foot Ulcers: A Double-Blinded Prospective Clinical Trial. *Int Wound J* **2023**, doi:10.1111/iwj.14186.
19. Lima, A.C.; Mano, J.F.; Concheiro, A.; Alvarez-Lorenzo, C. Fast and Mild Strategy, Using Superhydrophobic Surfaces, to Produce Collagen/Platelet Lysate Gel Beads for Skin Regeneration. *Stem Cell Rev Rep* **2015**, *11*, 161–179, doi:10.1007/s12015-014-9548-6.
20. Naskou, M.C.; Tyma, J.F.; Gordon, J.; Berezny, A.; Kemelmakher, H.; Richey, A.C.; Peroni, J.F. Equine Platelet Lysate Gel: A Matrix for Mesenchymal Stem Cell Delivery. *Stem Cells Dev* **2022**, *31*, 569–578, doi:10.1089/scd.2022.0097.
21. Mendes, B.B.; Gómez-Florit, M.; Babo, P.S.; Domingues, R.M.; Reis, R.L.; Gomes, M.E. Blood Derivatives Awaken in Regenerative Medicine Strategies to Modulate Wound Healing. *Adv Drug Deliv Rev* 2018, *129*, 376–393.
22. Marfoglia, A.; Tibourtine, F.; Pilloux, L.; Cazalbou, S. Tunable Double-Network GelMA/Alginate Hydrogels for Platelet Lysate-Derived Protein Delivery. *Bioengineering* **2023**, *10*, 1044, doi:10.3390/bioengineering10091044.
23. Xu, F.; Zou, D.; Dai, T.; Xu, H.Y.; An, R.; Liu, Y.; Liu, B. Effects of Incorporation of Granule-Lyophilised Platelet-Rich Fibrin into Polyvinyl Alcohol Hydrogel on Wound Healing. *Sci Rep* **2018**, *8*, doi:10.1038/s41598-018-32208-5.
24. Emami, F.; Vatanara, A.; Park, E.J.; Na, D.H. Drying Technologies for the Stability and Bioavailability of Biopharmaceuticals. *Pharmaceutics* 2018, *10*.
25. Budtova, T.; Aguilera, D.A.; Beluns, S.; Berglund, L.; Chartier, C.; Espinosa, E.; Gaidukovs, S.; Klimek-kopyra, A.; Kmita, A.; Lachowicz, D.; et al. Biorefinery Approach for Aerogels. *Polymers (Basel)* 2020, *12*, 1–63.
26. García-González, C.A.; Sosnik, A.; Kalmár, J.; De Marco, I.; Erkey, C.; Concheiro, A.; Alvarez-Lorenzo, C. Aerogels in Drug Delivery: From Design to Application. *Journal of Controlled Release* 2021, *332*, 40–63.
27. Zheng, L.; Zhang, S.; Ying, Z.; Liu, J.; Zhou, Y.; Chen, F. Engineering of Aerogel-Based Biomaterials for Biomedical Applications. *Int J Nanomedicine* 2020, *15*, 2363–2378.
28. Al Shehadat, S.; Gorduysus, M.O.; Hamid, S.S.A.; Abdullah, N.A.; Samsudin, A.R.; Ahmad, A. Optimization of Scanning Electron Microscope Technique for Amniotic Membrane Investigation: A Preliminary Study. *Eur J Dent* **2018**, *12*, 574–578, doi:10.4103/ejd.ejd_401_17.
29. Montemezzo, M.; Ferrari, M.D.; kerstner, E.; Santos, V. dos; Victorazzi Lain, V.; Wollheim, C.; Frozza, C.O. da S.; Roesch-Ely, M.; Baldo, G.; Brandalise, R.N. PHMB-Loaded PDMS and Its Antimicrobial Properties for Biomedical Applications. *J Biomater Appl* **2021**, *36*, 252–263, doi:10.1177/08853282211011921.
30. Terranova, L.; Louvrier, A.; Hébraud, A.; Meyer, C.; Rolin, G.; Schlatter, G.; Meyer, F. Highly Structured 3D Electrospun Conical Scaffold: A Tool for Dental Pulp Regeneration. *ACS Biomater Sci Eng* **2021**, *7*, 5775–5787, doi:10.1021/acsbiomaterials.1c00900.
31. Janmey, P.A.; Winer, J.P.; Weisel, J.W. Fibrin Gels and Their Clinical and Bioengineering Applications. *J R Soc Interface* 2009, *6*, 1–10.
32. Pinnow, M.; Fink, H.P.; Fanter, C.; Kunze, J. Characterization of Highly Porous Materials from Cellulose Carbamate. In Proceedings of the Macromolecular Symposia; January 2008; Vol. 262, pp. 129–139.
33. Weisel, J.W. FIBRINOGEN AND FIBRIN. **2005**, doi:10.1016/S0065-3233(04)70008-X.
34. Roberts, I.V.; Bukhary, D.; Valdivieso, C.Y.L.; Tirelli, N. Fibrin Matrices as (Injectable) Biomaterials: Formation, Clinical Use, and Molecular Engineering. *Macromol Biosci* 2020, *20*.
35. Zuo, L.; Zhang, Y.; Zhang, L.; Miao, Y.E.; Fan, W.; Liu, T. Polymer/Carbon-Based Hybrid Aerogels: Preparation, Properties and Applications. *Materials* 2015, *8*, 6806–6848.
36. Romn, J.; Cabãas, M.V.; Pẽa, J.; Vallet-Regí, M. Control of the Pore Architecture in Three-Dimensional Hydroxyapatite- Reinforced Hydrogel Scaffolds. *Sci Technol Adv Mater* **2011**, *12*, doi:10.1088/1468-6996/12/4/045003.
37. Harreld, J.H.; Dong, W.; Dunn, B. AMBIENT PRESSURE SYNTHESIS OF AEROGEL-LIKE VANADIUM OXIDE AND MOLYBDENUM OXIDE; 1998;
38. Book, G. IUPAC Gold Book;
39. Soorbaghi, F.P.; Isanejad, M.; Salatin, S.; Ghorbani, M.; Jafari, S.; Derakhshankhah, H. Bioaerogels: Synthesis Approaches, Cellular Uptake, and the Biomedical Applications. *Biomedicine and Pharmacotherapy* 2019, *111*, 964–975.

40. Peleg, M. The Instrumental Texture Profile Analysis Revisited. *J Texture Stud* 2019, *50*, 362–368.
41. Sung, Y.K.; Lee, D.R.; Chung, D.J. Advances in the Development of Hemostatic Biomaterials for Medical Application. *Biomater Res* 2021, *25*.
42. Babrnáková, J.; Pavliňáková, V.; Brtníková, J.; Sedláček, P.; Prosecká, E.; Rampichová, M.; Filová, E.; Hearnden, V.; Vojtová, L. Synergistic Effect of Bovine Platelet Lysate and Various Polysaccharides on the Biological Properties of Collagen-Based Scaffolds for Tissue Engineering: Scaffold Preparation, Chemo-Physical Characterization, in Vitro and Ex Ovo Evaluation. *Materials Science and Engineering C* **2019**, *100*, 236–246, doi:10.1016/j.msec.2019.02.092.
43. Babo, P.S.; Cai, X.; Plachokova, A.S.; Reis, R.L.; Jansen, J.; Gomes, M.E.; Walboomers, X.F. Evaluation of a Platelet Lysate Bilayered System for Periodontal Regeneration in a Rat Intrabony Three-Wall Periodontal Defect. *J Tissue Eng Regen Med* **2018**, *12*, e1277–e1288, doi:10.1002/term.2535.
44. García-González, C.A.; Sosnik, A.; Kalmár, J.; De Marco, I.; Erkey, C.; Concheiro, A.; Alvarez-Lorenzo, C. Aerogels in Drug Delivery: From Design to Application. *Journal of Controlled Release* 2021, *332*, 40–63.
45. Yasuhiko Tabata Tissue Regeneration Based on Growth Factor Release;
46. Johnson, K.E.; Wilgus, T.A. Vascular Endothelial Growth Factor and Angiogenesis in the Regulation of Cutaneous Wound Repair. *Adv Wound Care (New Rochelle)* **2014**, *3*, 647–661, doi:10.1089/wound.2013.0517.
47. Sahni, A.; Francis, C.W. Vascular Endothelial Growth Factor Binds to Fibrinogen and Fibrin and Stimulates Endothelial Cell Proliferation; 2000;
48. 14511467.
49. Andia, I.; Perez-valle, A.; Amo, C. Del; Maffulli, N. Freeze-drying of Platelet-rich Plasma: The Quest for Standardization. *Int J Mol Sci* 2020, *21*, 1–20.
50. Notodihardjo, S.C.; Morimoto, N.; Kakudo, N.; Mitsui, T.; Le, T.M.; Tabata, Y.; Kusumoto, K. Comparison of the Efficacy of Cryopreserved Human Platelet Lysate and Refrigerated Lyophilized Human Platelet Lysate for Wound Healing. *Regen Ther* **2019**, *10*, 1–9, doi:10.1016/j.reth.2018.10.003.
51. Liu, B.; Zhou, X. Freeze-Drying of Proteins. *Methods in Molecular Biology* **2015**, *1257*, 459–476, doi:10.1007/978-1-4939-2193-5_23.
52. Velnar, T.; Gradisnik, L. Tissue Augmentation in Wound Healing: The Role of Endothelial and Epithelial Cells. *Med Arch* 2018, *72*, 444–448.
53. Longhin, E.M.; El Yamani, N.; Rundén-Pran, E.; Dusinska, M. The Alamar Blue Assay in the Context of Safety Testing of Nanomaterials. *Frontiers in Toxicology* **2022**, *4*, doi:10.3389/ftox.2022.981701.
54. Niewiarowski, S.; Regoeczi, E.; Mustard, J.F. Adhesion of Fibroblasts to Polymerizing Fibrin and Retraction of Fibrin Induced by Fibroblasts1 (36425);